Magnetic Fields in Circumstellar Envelopes of Evolved AGB Stars

G. Pascoli

Université de Picardie Jules Verne, Faculté des Sciences, Département de Physique, 33 rue Saint-Leu, Amiens, Cedex F-80039, France; pascoli@u-picardie.fr

Abstract

In this paper, a time-dependent magnetohydrodynamic model is presented which aimed at understanding the superwind production by an evolved AGB star and the consecutive formation of a dense circumstellar envelope (CSE) around it. We know henceforth from various observations that a large scale magnetic field, probably toroidal in shape, is duly attested within these envelopes. Where does this large scale coherent field come from? The apparent antinomy between the quasi-round dense CSEs and their likely descendants, i.e., the elongated or bipolar Planetary Nebulae is also questioned. How is the spherical symmetry broken? We suggest in the present model that the nebula must effectively appear round during the superwind phase from the point of view of a distant observer. By contrast anisotropic structures are already appearing at the same time, but these ones remain hidden in the innermost regions. We predict thus the existence of a large bipolar cavity above the AGB star during the slow superwind phase. We then conjecture that the PPNe phase begins when the fast wind emitted by the core engulfs this cavity and increases the anisotropy of the distribution of gas. Thus even though paradoxically enough a beautiful evolved PNe can eventually emerge from a quasi-round dense CSE.

Key words: planetary nebulae: general – stars: winds, outflows

Online material: color figures

1. Introduction

The origin of magnetic fields in dense circumstellar envelopes (CSE) surrounding evolved AGB stars is still today a puzzling problem. The large number of observational studies contrasts with the fact that hitherto solely a few theoretical works are devoted to this topic (Pascoli 1987, 1992, 1997; Chevalier & Luo 1994; Matt et al. 2000; Blackman et al. 2001; García-Segura et al. 2005; Nordhaus et al. 2007; Nucci & Busso 2014). The well-posed problem is the following: the dense CSEs produced at the tip of the AGB stage possess weak expansion velocities, but a contrario, a large-scale magnetic field is presumably present. In the first case (weak expansion velocities) the progenitor must have a very large radius, which necessarily implies low rotational velocities; however in the second case (presence of a coherent magnetic field over large length scales) the rotation for the dynamo to be operating must be high. How can you solve this dilemma?

After leaving the main sequence low- and intermediate-mass stars, with an initial mass range of about 0.8–7$M_\odot$, reach the asymptotic giant branch (AGB). The total duration of the AGB phase is of the order of 10^5–10^6 yr. The AGB stars are powered by alternating burning of H and He in thin shells surrounding their inert C–O core (Busso et al. 1999). Very schematically this core is dense and very small with a radius of the order of 10^9 cm. It is surrounded by a very huge convective envelope with a radius of the order of 10^{13} cm. Mass-loss rates of AGB

stars, determined with various observational methods are typically in the range of 10^{-8}–10^{-5} $M_\odot$ yr^{-1} (Habing 1996). This is the now broadly accepted model of an archetypical AGB star (Höfner & Olofsson 2018).

However, in the present paper we look at a short interval of time of the full AGB stage. We are mostly concerned with the massive wind (the so-called superwind) produced during a late period of the AGB stage, namely at the tip of the AGB phase where mass losses as high as 10^{-4} $M_\odot$ yr^{-1} or even above, are measured (using for instance the OH 1612 MHz maser line observations of OH/IR stars). This period is very short, of the order of 10^4 yr. Such a massive wind eventually produces a dense CSE with density typical of that observed in protoplanetary nebulae (PPNe) and planetary nebulae (PNe) (Herwig 2005; Höfner & Olofsson 2018). It is important to specify that these CSEs are characterized by both relatively weak asymmetries at a large scale and a low velocity field ~ 10 km s^{-1} (Kerschbaum et al. 2010). However, the observations of their immediate descendants, namely the PPNe often exhibit high velocities associated to a strong bipolarity. This drastic change is rather intriguing (Duthu et al. 2017). This is the topic of the present paper to explain how a very complex structure, i.e., a structure composed of an inner disk or a torus, surrounded by a bipolar inner structure, itself surrounded by an outer spherical envelope, can be produced.

Pascoli (1997) hypothesizes that the primary cause of the ejection of massive winds by an evolved AGB red giant would

possibly be the magnetic activity present just above its degenerate core. The transportation of magnetic field from the dense core to the stellar surface is entirely ensured by turbulent diffusivity and, de facto, the modelization was depending on an arbitrary constraint, that is that the macroscopic meridional velocity is zero within the star (self-imposed in a one-dimensional model for which there exists no possiblity to set up a countercurrent flow). A major difficulty with this model is that magnetic stresses have a smoothing effect on the angular velocity gradient and the dynamo is eventually quenched. In fact, this problem resides in the zero-meridional circulation hypothesis. However, if the arbitrary constraint of zero meridional velocity is relaxed, the situation changes drastically. Then a bidimensional analysis was needed.

Nordhaus et al. (2007) have succeeded in developing much more sophisticated 2.5 dimensional models than the one-dimensional model of Pascoli (1997). The counter-reaction of the magnetic field on the differential rotation is explicitly considered in these models. The aim of these authors was to know if a single star can produce a magnetic field over a sufficient period of time to eject and to adequately shape a PN. Their conclusion is that there exists a possibility if a convection reseeds the angular momentum in an efficient manner. These authors briefly examine this question in their Section 2.4. Unfortunately no detailed calculations are presented and no definitive conclusion can be brought. There exist indeed various types of convections and some them can even destroy the dynamo. The only star where a sustaining–dynamo convection is well studied is the Sun. In this star a global convection is existing in the form of a meridional circulation. This circulation acts as a conveyor belt and is a key ingredient in the magnetic activity of the Sun (Kitchatinov 2016). Following this author: The meridional flow can be defined as a poloidal part of the global axisymmetric motion resulting from an averaging—over time or longitude or ensemble of convective motions—of the velocity field. Without a well adapted self-organized meridional circulation the dynamo cannot efficiently run over a long period. This mechanism has a dual role: first to bring fresh angular momentum toward the region where the dynamo resides and second to drain the newly created magnetic field for preventing it to quench the dynamo.

The second role is of great importance, the dynamo cannot run if the newly magnetic field in not quickly evacuated from the dynamo zone. However, it has long been known that a magnetic field cannot disengage from the star if it is diffuse. For that it must first be concentrated (Parker 1984). Nordhaus et al. (2007) do not address this issue.

In this vein, Pascoli & Lahoche (2008, 2010) discussed the conditions of ejection by an evolved AGB star in the framework of an axisymmetric magnetohydrodynamic model. A strong toroidal magnetic field is produced by a dynamo mechanism in the core region of the star. The magnetic field

effectively tends to brake the rotation in the core region but this effect is now counterbalanced by a supply of new angular momentum from the higher latitudes and a steady state can be achieved. These authors have also shown that the AGB's atmosphere and the ejected CSE are not really separable, but should be treated as a continuous mass distribution. However, a steady state model is not fully predictive in the sense that the solution is very generally ab initio-induced and the equations are simply checked. A much better approach is to take a time-dependent model and to start from the ending stage of contraction of the core of an AGB star, assuming no circulation and no toroidal magnetic field at the beginning of computations. Then we can analyze how these quantities can spontaneously develop in a self-consistent manner. This issue is explored in the present paper in the framework of time-dependent simulations. The procedure follows the usual appoach of mean-field electrodynamics (Krause & Rädler 1980; Rüdiger & Hollerbach 2004; Charbonneau 2010).

Another difference with the model of Pascoli and Lahoche is that the rotation profile is now found to have a polar and not an equatorial structure. Contrarily what we usually think, it is not so difficult to create a high magnetic field $\sim 10^6$ Gs in the core region of an evolved AGB star. The problem is rather how to maintain the dynamo in a steady state for say here 10^4 yr (the duration of the superwind ejection with a consecutive CSE formation). If the new field is not rapidly evacuated, it back-reacts on the dynamo and the differential rotation is spreaded out. The idea is to imagine that the field is built-up in a region (the so-called dynamo region) and the compression of the field takes place in another one. Another problem is linked to the evacuation of the field which must be sufficiently rapid so that a balance is established between creation and loss. This time the field is created by a polar dynamo instead of an equatorial one. The magnetic field is then strongly compressed in the equatorial plane. Thus the highly magnetized area and the dynamo area become distinct. The novelty here is that now the action of a high magnetic field does no longer hinder the dynamo in a natural way.

Large-scale magnetic fields in PPNe and PNe were also hypothesized by a lot of authors in order to explain the rather remarkable morphologies (Gurzadyan 1969; Pascoli 1987, 1992, 1997; Chevalier & Luo 1994; Matt et al. 2000; Blackman et al. 2001; García-Segura et al. 2005). The origin and the effects of magnetic fields in the progenitor were also considered (Nordhaus et al. 2007, 2008; Blackman 2009; Nucci & Busso 2014). This paradigm has been considerably strengthened by observational data of CSEs of evolved carbonaceous stars—the assumed ancestors of PPNe and PNe —(Vlemmings et al. 2005; Herpin et al. 2006; Sabin et al. 2007; Kemball et al. 2009; Vlemmings 2012; Lèbre et al. 2014; Sabin et al. 2015; Duthu et al. 2017), but also by laboratory experiments (Ciardi et al. 2009).

Some authors have also pointed out the indirect signature of underlying magnetic fields in PNe by the presence of a large coherent network of filaments (Huggins & Manley 2005). The matter which composes a filament is naturally oriented following a directional bundle of magnetic field lines and can preserve its coherence over very long distances (comparable to the diameter of the nebula), and these filaments are generally twisted. A typical case is NGC 3132 where we can very distinctly see a prominent straight chord composed of two interlacing filaments starting from a rim and going to the opposite one of the nebula, see the Figure 2 of the paper by Huggins & Manley. (Is it posssible to produce similar structures, i.e., connected on very long distances, from simple hydrodynamic, shearing instabilities or shocks?)

On the other hand an important point to notice is that if a large-scale magnetic field is existing in the dense CSE produced at the very end of the AGB stage (which is characterized by a very high mass loss rate $\sim 10^{-4}\ M_\odot\ \mathrm{yr}^{-1}$), then this field must necessarily still exist in its descendant, i.e., a PPN. In other words to observe a large-scale coherent magnetic field in dense CSEs of evolved AGB stars implicitely leads to admit its presence in PPNe (Duthu et al. 2017).

We can add that a large scale coherence of the magnetic field in the CSEs signifies that this field has been created in a very small region (very likely the core of the evolved AGB star where the rotation is presumably high) and then extended at a large scale by expansion of the gas derived from the star (it appears very difficult indeed, if not impossible, to directly create a coherent magnetic field over a large scale).

Another very interesting but different topic to be addressed in the present paper is why the CSEs generally appear grossly round at a large scale (Neri et al. 1998; Kerschbaum et al. 2010), while otherwise their descendants (PPNe and evolved PNe) very often appear strongly bipolar or at least highly axisymmetric.

2. The MHD Equations

We assumed axisymmetry and spherical coordinates (r, θ, ϕ) are used in all our calculations.

The continuity equation is:

$$\frac{\partial \rho}{\partial t} + \nabla.(\rho \boldsymbol{v}) = 0 \tag{1}$$

where ρ denotes the mass density and $\boldsymbol{v}$ the velocity of gas.

The momentum equation reads:

$$\frac{\partial \boldsymbol{m}}{\partial t} + \nabla.\left(\boldsymbol{m}\boldsymbol{v} - \frac{1}{4\pi}\boldsymbol{H}\boldsymbol{H}\right) + \left(P + \frac{H^2}{8\pi}\right)1 = \nabla.\pi - \rho\boldsymbol{g} \tag{2}$$

In this expression $\boldsymbol{m}$ is the momentum density ($=\rho\boldsymbol{v}$), p is the thermal pressure P ($=\frac{\rho k_B T}{\mu m_H}$ with k_B the Boltzmann constant, T the temperature, $\mu = \frac{1}{2}$ and m_H the atomic unit mass). The

isotropic viscous stress tensor π which is given by

$$\pi = \rho\nu\left[(\nabla \boldsymbol{v} + (\nabla \boldsymbol{v})^T + \frac{1}{3}\nabla.\boldsymbol{v}1\right]$$

(ν denotes the turbulent viscous transport coefficient, 1 the unit tensor)

The gravitational acceleration vector $\boldsymbol{g}$ is taken equal to $-\frac{GM(r)}{r^2}\frac{\boldsymbol{r}}{r}$. The gravitational mass $M(r)$ of the envelope evaluated at the distance r is calculated with the relationship:

$$M(r) = M_c + 4\pi \int_{r_c}^{r} \overline{\rho}(r')r'^2 dr' \tag{3}$$

where M_c expresses the degenerate core mass and $\overline{\rho}(r)$ designates the averaged-over-latitude density. The energy equation may be written in the form (see, e.g., Dobler et al. 2006):

$$\frac{\partial E}{\partial t} + \nabla.\left[\left(E + P + \frac{H^2}{8\pi}\right)\boldsymbol{v} - \frac{1}{4\pi}\boldsymbol{H}(\boldsymbol{v}.\boldsymbol{H})\right]$$
$$= \nabla.\left[(\pi.\boldsymbol{v}) - \frac{\eta}{4\pi}(\nabla \wedge \boldsymbol{H}) \wedge \boldsymbol{H} + \kappa\nabla T\right] + \boldsymbol{m}.\boldsymbol{g} \tag{4}$$

where T denotes the temperature, κ represents the thermal conduction coefficient.

Eventually the kinematic axisymmetric dynamo equation is (Dikpati & Charbonneau 1999; Charbonneau 2010):

$$\frac{\partial \boldsymbol{H}}{\partial t} + \nabla \wedge (-\boldsymbol{v} \wedge \boldsymbol{H}) = -\nabla \wedge (\eta\nabla \wedge \boldsymbol{H} - \alpha\boldsymbol{H}) \tag{5}$$

where η is the turbulent magnetic diffusivity ($\eta = \frac{1}{3}\tau\overline{\boldsymbol{u}^2}$ with τ the correlation time for the turbulence and $\boldsymbol{u}$ the turbulent velocity).

The source term on the right-hand side $\alpha\boldsymbol{H}$ ($\alpha = -\frac{1}{3}\tau\overline{\boldsymbol{u}.\nabla \wedge \boldsymbol{u}}$) expresses the regeneration of the field by isotropic α-mechanism (see, Dikpati & Charbonneau 1999; Charbonneau 2010).

3. Computational Details

All the calculations were performed using the PLUTO package (Mignone et al. 2007, 2015) implemented on a SGI Altix UV100 computer. This program is a finite-volume/finite-difference, shock-capturing code designed to integrate a system of MHD-equations in the form of conservative laws (the MHD equations given above are discretized using this form). Flux computation has been made employing the hhlc (Harten, Lax, Van Leer) Riemann solver. The RK3 time-marching algorithm was used. The domain under study is extended from 10^9 to 3×10^{15} cm. This domain is thus divided in three subdomains:

(a) The core (dynamo) region from $r_c = 10^9$ to 3×10^{12} cm. For this area, the various timescales at stake are very different: the dynamical timescale ~ 3 s, the rotational period ~ 600 s, the characteristic time of the meridional circulation $\sim 10^3$ s and eventually the characteristic times of diffusion and regeneration

of the poloidal field from the azimuthal component, both $\sim 10^5$ s.

(b) The transition area from 3×10^{12} cm to $r_\star = 3 \times 10^{13}$ cm.

(c) The CSE from 3×10^{13} cm to $r_\infty = 3 \ 10^{15}$ cm.

These three domains form a single one, but this arbitrary division is imposed by the characteristic time of evolution which is once again different for each of these regions. It is thus important to notice that such a division is a practical way to greatly shorten the CPU time (by reducing it to only a few months!). This division results from a numerical treatment but does not necessarily express a physical reality. An ideal situation would obviously be to treat these three zones as an unique one, but the latter procedure would need a very big supercomputer.

The parameters:

We have assumed that the turbulence (velocity v_t) is exalted in the vicinity of the core (radius r_c):

$$v_t = v_{tc} \left(\frac{r_c}{r} \right)^{1/2} + v_{te}. \qquad (6)$$

Exaltation of the turbulence is predictable taken account of the impinging stream of matter at the base of the convective envelope, this stream resulting from the descending polar column linked to the contraction of the inner region at a final stage.

The parameter v_{tc} ($=5 \times 10^5$ cm s^{-1}) represents the turbulent velocity taken at the core surface and v_{te} ($=10^5$ cm s^{-1}) is the turbulent velocity throughout the evolved AGB's envelope.

The α-ffect (restricted to the isotropic case) is modeled by the closed-form function:

$$\alpha = \alpha_c \frac{1}{1 + \left(\frac{H}{H_{eq}} \right)^2} \left(\frac{r_c}{r} \right)^{1/2} \cos \theta \qquad (7)$$

with $\alpha_c = 10^4$ cm s^{-1} and the equipartition value $H_{eq} = \sqrt{4\pi\rho}$ v_t. This effect is responsible for the production of magnetic fields by α process as admitted in the framework of the mean-field dynamo theory. The quenching factor $1 + \left(\frac{H}{H_{eq}} \right)^2$ in the denominator underlies that the Lorentz force associated with the dynamo-generated magnetic fields impedes the turbulent fluid motions. This term ensures that the poloidal field generation process is stopped when the toroidal component is close to -or higher than- the equipartition value H_{eq} (see, e.g., Küker et al. 2001). The other factors, that is the $\cos\theta$ latitude profile and the exponential r-dependence, are of common use in the mean-field dynamo models where they appear as simple geometric cutoffs (see, for instance, Chatterjee et al. 2004; Charbonneau 2010).

Similarly, we define the profile of η by the expression:

$$\eta = \eta_c \frac{r}{r_c} \frac{v_t}{v_{tc}} \frac{1}{1 + \left(\frac{H}{H_{eq}} \right)^2} \qquad (8)$$

where $\eta_c = 10^{13}$ cm^2 s^{-1} (magnetic Reynolds number $R_m \sim 100$).

As mentioned above, the term $\frac{1}{1 + \left(\frac{H}{H_{eq}} \right)^2}$ represents the η-quenching as due to the nonlinear magnetic field feedback on the turbulence. The H-dependence of η introduces a dose of nonlinearity in the problem. A quite similar factor is used in the solar dynamo theory (Dikpati & Charbonneau 1999; Gilman & Rempel 2005; Charbonneau 2010). The $\frac{r}{r_c}$ factor traduces the reasonable hypothesis that the mixing length linearly increases with r in the evolvd AGB's envelope (Pascoli 1997). The present calculations thus fully assume that the MHD physics available for the Sun is immediately transposable to evolved AGB's stars. It is difficult to say if it is effectively the case, but it seems that this physics appears universal and applies to all structures in the universe, whatever the characteristic length of the object under examination (more specifically all types of stars) is. These considerations are general and have also been developed outside the strict solar domain (Beck et al. 1996).

We admit that the magnetic Prandtl number $P_r = \frac{\nu_c}{\eta_c} = 1$. All these parameters have dimensions of $L \times V$, or numerically can be estimated $\sim 0.3 l_c v_{tc}$ with l_c turbulent correlation length) (Pascoli & Lahoche 2008, 2010). However, other choices can still be made (see for instance Nucci & Busso 2014).

The pertinence of the values chosen for the adjustable parameters A_c and (η_c, α_c) must lead to agreement with the observational data, especially here the measurable quantities, i.e., mass loss, expansion velocity and flux loss produced by the evolved AGB stars during the slow superwind phase. This statement does not vindicate the model in itself but at least shows that, within its explanatory framework and with realistic numerical values for these parameters, we can obtain the good values for the observable quantities. (As in other similar MHD problems, for instance in the dynamo models for the Sun, where the aim is to obtain the best fit to observed solar cycle.)

In order to solve the system of equations, the initial conditions have still to be specified. We have chosen a simplified model of evolved AGB star.

The total mass of the star $M_\star = M_c + M_{env}$ is taken equal to one solar mass, with a core mass equal to $0.5 \, M_\odot$ ($r_c = 10^9$ cm) and a mass for the convective envelope equal to $0.5 \, M_\odot$ ($r_\star = 3 \times 10^{13}$ cm).

The initial density and temperature in the evolved AGB's envelope is taken by solving the equilibrium equation (assuming both spherical symmetry and no macroscopic

motion in the convective envelope):

$$-\frac{GM(r)\rho(r)}{r^2} - \frac{\partial P}{\partial r} = 0. \qquad (9)$$

We have assumed that the matter composing the convective envelope is essentially an ideal gas with negligible radiation pressure. This approximation appears legitimate at an average point of the envelope, even though this one becomes false just above the CO core (more precisely the base of the convective envelope). In spite of this we have put $P \equiv P_{\text{th}}$ everywhere in the convective envelope (after noticing that, approximately, $P_{\text{th}} \sim r^{-\frac{5}{2}} \gg P_{\text{rad}} \sim r^{-4}$). This trick (associated to many other drastic simplifications made in this work!) helps to save CPU time which still remains very long. In fact the essential problem is numerical. The consideration of the radiation pressure creates a much higher gradient of density above the core surface and the numerical mesh has to be considerably reduced (increasing the CPU time).

We admit that this subterfuge should not affect the dynamo too much. On the contrary we may think that the consideration of the radiation pressure would allow to increase the density (and the pressure) above the CO core position (compared to the values taken in our model) and thus to still minimize the harmful back-reaction on the differential rotation (the source of the field).

That being said, the pressure–density–temperature relation is here the usual ideal law $P = 2\frac{\rho}{m_H}k_B T$, available for a fully ionized medium composed of pure hydrogen. The density and temperature at $r_c = 10^9$ cm are respectively $\rho_c = 0.1$ g cm^{-3} and $T_c = 1.5\ 10^8$ K.

We must also specify that what is considered here as the base of the convective envelope is not directly identified with the CO core surface. The region just above the inert CO core (radius $r_c = 10^9$ cm) is indeed the seat of very complex nucleosynthesis processes. We find there a thin double sheet consisting in a He-burning shell surrounded by a H-burning shell. These two thin sheets, which can alternatively be active or not, are separated by an intershell consisting of a mixture of He, C with a few percent of ^{22}Ne and O (Busso et al. 1999; Herwig 2005; Karakas & Lattanzio 2014). What is named here "base of the convective envelope" is located just above this double sheet. Let us note that the inner zone, i.e., the inert CO core and the He and H burning shells on top of it, do not intervene in the specific scenario envisioned here, that is the build-up of a toroidal magnetic field at the base of the convective envelope, its transport through this envelope and eventually its ejection accompanied by a strong mass loss at the AGB surface. If, possibly, there exists a core dynamo, this one is then assumed to be fully disassociated from that described in the present paper. The magnetic field considered here is not anchored on the CO core surface. This will be discussed further below.

At the "stellar surface" the boundary conditions are $M(r = r_\star) = M_\odot$, $\rho(r = r_\star) \sim 10^{-11}$ g cm^{-3} and $T(r = r_\star) = 3000$ K. These values are slightly different from those chosen for instance by Nucci & Busso (2014), but it must be remembered that they are arbitrary (the surface of an evolved AGB star is not a geometric surface perfectly defined. It is rather a "volume" with an thickness of $\sim 3 \times 10^{12}$ cm. For the region of emission of the slow superwind, there is not even any surface at all, but a continuum between the "star" and an outer thick disk).

4. Results

The output data (with format .vtk) have been visualized using the open source package VisIt (version 2.10) distributed by the Lawrence Livermore National Laboratory.

a. The core region

We name here by "core region" the zone located just above the system composed of the inert CO core crowned by the H-He double sheet. It is in fact the deepest part of the convective envelope. The rotation profile within this region is an essential data for the dynamo models. This is indeeed the differential rotation which insures the build-up of the magnetic field in this region. Retrospectively the present model could thus help to fix the initial conditions for the rotation and the magnetic field in the core region of an evolved AGB star.

Fortunately even though the Sun and an evolved AGB star are two very different stars, the Sun will evolve in an evolved AGB and it appear reasonable to assume that some imprint seen in the rotation profile of the Sun will still exist at the evolved AGB stage (not least by angular momentum conservation). The Heliosismology produces the internal differential rotation profile of the Sun. The physical conditions reigning at the surface of the Sun are equally known. In the Sun the angular rotation is quasi uniform with a value at the surface of the order of 2×10^{-6} s^{-1}. We take at $r = 10^{11}$ cm $\Omega_{11} \sim 2 \times 10^{-6}$ s^{-1}. This numerical value appears reasonable. Concerning the solar core region recent measurements of the rotation rate by identification of asymptotic gravity modes (GOLF instrument on board *Solar and Heliospheric Observatory*; *SOHO*) (Fossat et al. 2017) seem to contradict the preceding values obtained by BISON (Patern et al. 1996). If the results of Fossat et al. are confirmed the angular velocity of the solar core would be much higher than at the surface (by a factor 4), increasing at the same time the available total angular momentum. Obviously the value observed at the surface is left unchanged.

We do a similar reasoning for the magnetic field. For the Sun the observed magnetic flux is of the order of 10^{23} Mx. For a radius of the order of 10^{11} cm this gives a mean magnetic field of 1 Gauss. A series of preliminary runs shown that this initial magnetic field concentrates in the polar area with conservation of flux. This eventually gives an estimate of ~ 10 Gs for the magnetic field for the latitudinal angle $\theta = 5°$–$30°$. We have

then started our calculations with a guess entry for the magnetic field intensity imposing a value of 10 Gauss at say $r_{11} = 10^{11}$ cm for the latitudinal angle θ lying between 5° and 30°.

In our preceding work (Pascoli & Lahoche 2010) the model was steady and we taked the boundary conditions (magnetic field and rotation) at the surface of the core. Instead, here, the model is time-dependent and the boundary conditions (magnetic field and rotational velocity) are taken at $r_{11} = 10^{11}$ cm. This procedure now appears much more natural because this is the sense of the meridional circulation which carries the angular momentum from the outer polar regions toward the base of the convective envelope (the radius of this base is labeled r_c in the following). The distribution of angular velocity is thus modelized from that of the Sun after contraction of the central region, i.e., with respect to the analytic formula $\Omega(r, \theta) = \Omega_c\left(\frac{r_c}{r}\right)^2$ (obeying to the law of angular momentum conservation with variation in r^{-2} during the contraction of the core). In this context the angular velocity at the surface of the evolved AGB star is very weak $\sim 10^{-9}\,\mathrm{s}^{-1}$ or $v_{\mathrm{eq}} \sim 0.3\,\mathrm{km\,s}^{-1}$ (equatorial value for the azimuthal velocity), while near the base of the convective envelope $\Omega_c \sim 10^{-2}\,\mathrm{s}^{-1}$ or $v_{\mathrm{eq}} \sim 100\,\mathrm{km\,s}^{-1}$. This quantity is a key parameter of the model. We can remark that the mean equatorial velocity of the white dwarfs is sensibly weaker $\lesssim 20\,\mathrm{km\,s}^{-1}$. We thus implicitly assume that the region surrounding the core of an evolved AGB star rotates more rapidly than a white dwarf and/or still that it is this core itself which slows down during the envelope ejection (by magnetic coupling but a very high magnetic field is needed). May be can we eventually imagine more simply that the degenerate core rotates more slowly that the base of the evolved AGB's envelope, where the magnetic field under consideration here is generated. We can suggest a vague analogy with the superrotation of the Venus atmosphere which rotates much speeder than the planet itself, even though in this case the latter phenomena appear in another very different context and have of course a distinct origin (planetary polar vortices has also been found in the solar system, however, the mechanism which maintains them seems a delicate balance between warming and cooling in the atmosphere. On the other hand as due to very low conductivity no dynamo (and no magnetic field) is associated to these vortices).

As for the magnetic field we start with a mixed extended dipole-quadrupole poloidal component represented by the potential vector (a seed of field is needed to get the dynamo started):

$$A_\varphi(r, \theta) = A_{11}[1 - \exp-e^{-(\frac{r - r_c}{0.1 r_c})}]$$
$$\left[0.1\left(\frac{r_{11}}{r + r_{11}}\right)\sin\theta + 0.9\left(\frac{r_{11}}{r + r_{11}}\right)^3 \sin\theta\cos\theta\right]. \quad (10)$$

The boundary conditions at $r \sim 10^{11}$ cm are $H_r = -10$ Gs for $\theta = 5°$–30° and $= 0$ for $\theta = 0°$–5° and 30°–90° (and the same thing in the south hemisphere by symmetry but with $H_r = -5$ Gs). The constant $A_{11} \sim 6 \times 10^{12}$ Gs m is estimated from the value at $r \sim 10^{11}$ cm.

Let us notice that the magnetic field value measured by Jordan et al. (2005) at the surface of a small number of central stars of PNe (the evolved remnant of the evolved AGB's core), that is of the order of 10^3 Gauss, does not intervene in this initial conditions (we avoid to fix the boundary conditions for the magnetic field at $r = r_c$ which are unknown). The values of Jordan et al. are measured at the surface of the central star of PNe, not at the surface of the core of an evolved AGB star (where this measurement is definitely not possible). If there exists a magnetic field built-up by the degenerate core, it is very likely disconnected from this one which is considered here and which is produced at the base of the evolved AGB's envelope. In any way and after new observations the intensity of the magnetic field measured at the surface of central stars (the bare core) of PNe seems weak ($\lesssim 1$ kGs, see Jordan et al. 2012). Paradoxically enough some white dwarfs ($\sim 10\%$) have a surface field ranging from 10^3 up to 10^9 Gs. However, for high magnetic values, field generation within the common envelope of a binary stellar system has been suggested (with production of a complex and non-dipolar structure exhibiting the presence of higher order multipoles) (Ferrario et al. 2015).

Concerning the dipole component, this one plays a minor role and could eventually be suppressed. This component forms two sheets of opposite signs in the equatorial plane where finally it annihilates. Besides it creates an north–south asymmetry between the two hemispheres. Sole the quadrupolar component contributes to the formation of the magnetized equatorial disk. In any way the initial conditions taken for the field are not very significant because this field is strongly reshuffled by the meridional circulation toward the pole.

We have started the calculations with the initial conditions supplied above. No meridional circulation and no toroidal magnetic component is assumed to be present.

Especially important is the root cause of a one-cell meridional circulation which appears in the convective envelope (we know that a similar phenomenon is existing in the Sun and which extends from the tachocline up to the surface, see Liang et al. 2018). In the present model, we are mainly concerned by the apparition of such a circulation but at the tip of the AGB phase (the stage where the AGB becomes a so-called OH/IR star). Very likely this self-organized motion starts in a zone located above the CO core—double H–He burning shell system and then extends over the totality of the convective envelope. The causes of a locking of chaotic small-scale motions in an organized mode at a large scale can be numerous (Kitchatinov 2016). We can indeed invoke an ultimate slight core contraction which can reinforce the
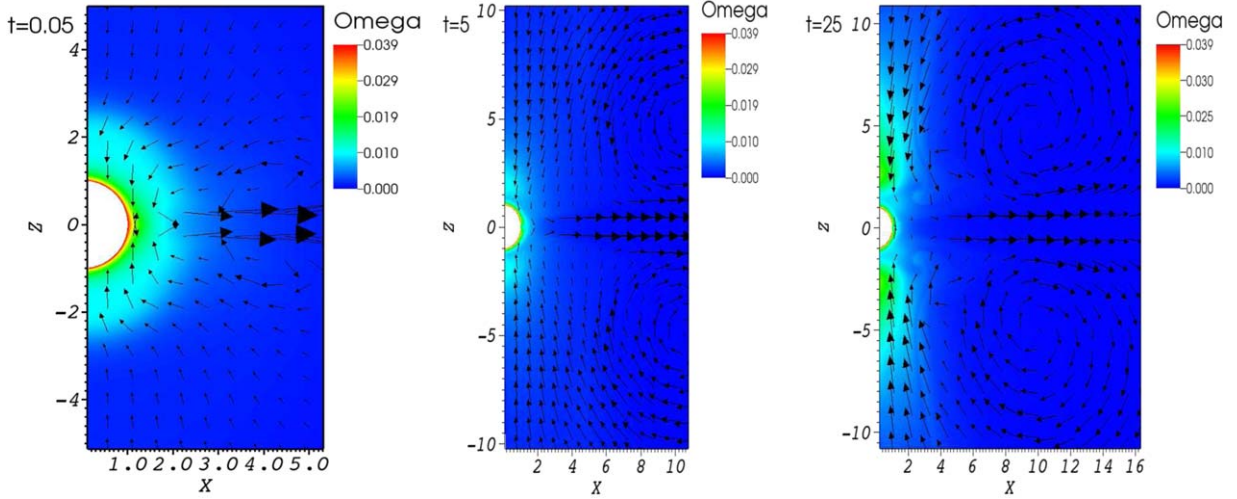
Figure 1. Core region: angular velocity in normalized units, unit $= 3 \times 10^8$ km s^{-1} (log scale). The meridional velocity field is surimposed (characteristic velocities ~ 5 km s^{-1}). The time unit is 5 hr.

(A color version of this figure is available in the online journal.)

rotation, a gradient of temperature or still a gradient of chemical abundance between the equator and the pole. In fact very small effects can produce a large-scale circulation. In the following we favor the simple process of a slight core contraction (with a consecutive increase of the rotation in the core region) for the initiation of the meridional circulation. The driving of a meridional flow by centrifugal forces is long known (Kitchatinov 2016). Let us note that in the Sun the apparition and the persistence of the meridional circulation in the convective zone is also a problematic area. In the MHD models for the Sun the meridional circulation is directed by the inconspicuous introduction at the beginning of the calculations of a lot of fine-tuned parameters, analytic formulae, etc. (e.g., Dikpati et al. 1995; Charbonneau 2010; Kitchatinov 2016). The same procedure is used in in other stars (Dobler et al. 2006). However, very interestingly, we will see later that, once formed, this meridional circulation coupled to the differential rotation in turn triggers the production of a strong toroidal magnetic field which ultimately leads to a very high mass loss by the star.

We assume thus here that the final stage of contraction of the central regions triggers an amplification of the angular velocity above the inert CO core. Our numerical simulations show that this phenomenon is spontaneously accompanied in its turn by the formation of vortices with strong mean velocities ($\sim 5 \times 10^5$–10^6 cm s^{-1}). A surimposed large scale meridional circulation also appears but with low mean velocities ($\sim 10^5$ cm s^{-1} at $r = 10^{11}$ cm). We can notice that this large scale flow is not here assumed by using an adhoc streamline function like in most solar models (Guerrero et al. 2005; Charbonneau 2010; Pipin & Kosovichev 2011; Nucci & Busso 2014), but its directly results

from computations (the initial conditions at $t = 0$ assume no meridional circulation). Even though the procedure is extremely time-consuming, here the velocity field is not chosen in advance and the model is self-consistent. We note that the meridional velocities calculated here $\sim 10^5$ cm s^{-1} at $r = 10^{11}$ cm are much higher than that measured at the surface of the Sun, $\sim 10^3$ cm s^{-1}. However, the centrifugal excitation is also much higher here and is appears natural that the meridional circulation be exalted. A single cell is generated by hemishere (this statement seems also favored in the convective area of the Sun, as suggested by *SOHO*/MIDI and *SDO*/HMI observations, but there exists other possibilities (see Liang et al. 2018), even though such an analogy must obviously be taken with cautious being the Sun and an evolved AGB star are very different in their structure).

At the beginning of calculations ($t \sim 0.25$ hr is of the order of the period of rotation of the degenerate core) the dynamo is both equatorial and polar (the Figure 2(a) shows the beginning of the magnetized disk formation). However, the equatorial dynamo produces a weak azimuthal transient field with an opposite polarity, which rapidly disappears while the polar contribution goes down to the equator and becomes rapidly dominant by compression.

After a duration $\gtrsim 1$ hr, examination of Figure 1(b) shows that the initial angular rotation has been deeply reshuffled by the meridional circulation. It is now largely "antisolar," i.e., very fast at higher latitudes (the pole region), but much slower near the equator as due to the strong magnetic breaking (Figure 1(c)). Modifying by a factor 2 or 1/2 the key parameter of the model, that is the initial angular velocity at $r = 10^{11}$ cm, Ω_{11}, does not change this situation.
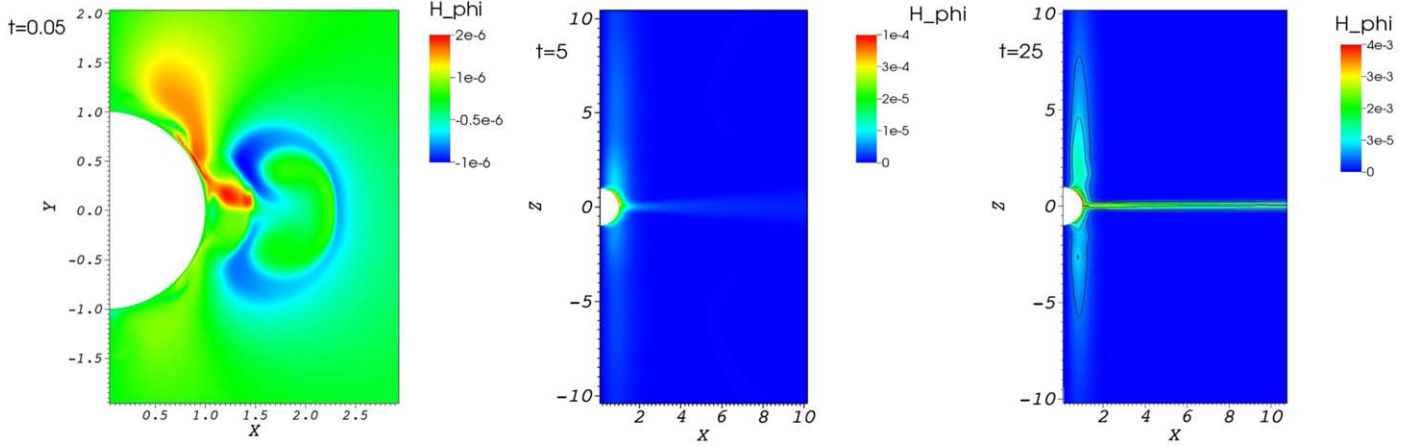
Figure 2. Core region: azimuthal magnetic field in normalized units, unit $= 7 \times 10^8$ Gs (Figure 2(a) linear scale, Figures 2(b), (c) log scale). The time unit is 5 hr. (A color version of this figure is available in the online journal.)

Quasi-simultaneously, the toroidal magnetic field component is generated from the poloidal field at higher latitudes ($\gtrsim 60°$) as due to shearing by axisymmetric differential rotation or ω-effect (Figures 2(b), (c)). The meridional vortices have then a rolling mill action which squeezes and amplifies, with constant magnetic flux, the magnetic field toward the equatorial plane where it is finally stored forming a strongly magnetized disk. We can thus notice that the process protects the differential rotation which is located at higher latitudes against spreading by the Lorentz forces, the dynamo region and the storage area being distinct. The built-up of toroidal vortices and magnetic buoyancy are not interlinked (we recall that the toroidal vortices are already present before the built-up of a significant magnetic field, in other words the meridional circulation appears first and then after the azimuthal component of the magnetic field is created. This result was not accessible in the preceding model of Pascoli and Lahoche where the dependence in time was not taken into account). In addition, the equatorially concentrated flux loss from the dynamo region is the dominating field-limiting process for the dynamo (by contrast, the magnetic diffusivity in the polar column has just a smoothing role). Likewise the gas in the thin magnetized disk is dragged by buoyancy and flux ropes present in this disk float upwards.

After a time of the order of a few hours the initial configuration of the magnetic field has thus been deeply transformed by the meridional circulation. The rotation is now essentially polar and the poloidal magnetic field is also largely concentrated in a polar column within an angle $30°$ (Figure 3). Let us note that the boundary condition $v_r = 0$ at $r = r_c$, $\theta = 0°$ (the core is assumed to be impenetrable) imposes that a static column is necessarily present above the core within an angle $\lesssim 5°$ with no field. In the polar column the magnetic field
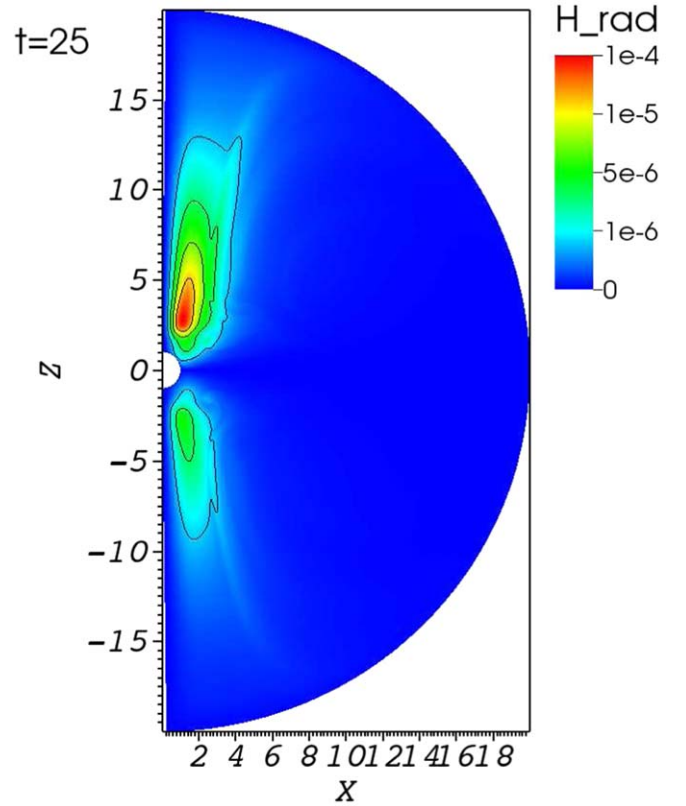

Figure 3. Core region: radial magnetic field in normalized units, unit $= 7 \times 10^8$ Gs (log scale).
(A color version of this figure is available in the online journal.)

is azimuthal just above the core and quasi-radial at a large distance (Figure 4).

Once installed the rotation field does not longer vary because the magnetic torque remains weak. The equilibrium value for
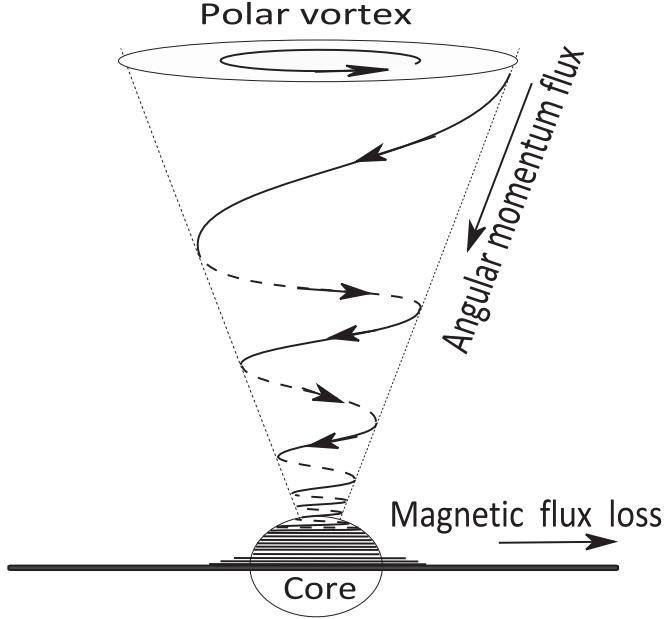
Figure 4. Sketch of an idealized dynamo-generated magnetic flux above the core region inside an evolved AGB star.

this torque is (near the core)

$$(H_r H_\varphi)_{\rm eq} \sim 4\pi (\rho v_r v_\varphi)_c \qquad (11)$$

or evaluating the right member $\sim 10^{14} \gg (H_r H_\varphi)_c \sim 10^{11}$. Fitting laws for the physical quantities[1] in the polar dynamo column for $r > 1.2 r_c$ and $5° \leqslant \theta \leqslant 30°$ are (the flow is quasi-radial and the poloidal magnetic field is practically reduced to its radial component):

$$v_r \sim r^{-1/2} \quad \Omega = \Omega_c \left[\left(\frac{r_c}{r} \right)^2 - \alpha \left(\frac{r_c}{r} \right)^{7/2} \right] \qquad (12)$$

with $\alpha = \frac{(H_r H_\varphi)_c}{(4\pi(\rho v_r v_\varphi)_c)} \sim 10^{-1}$ and

$$H_r \sim r^{-2} \quad H_\varphi \sim r^{-5/2} \qquad (13)$$

and

$$\rho \sim r^{-3/2} \quad T \simeq T_c \left[(1 + \beta) \frac{r_c}{r} + \gamma \left(\frac{r_c}{r} \right)^{7/2} \right] \qquad (14)$$

with $\beta = -\frac{1}{10} \frac{m v_c^2}{k T_c} \sim 10^{-5}$ and $\gamma = -\frac{3}{10} \frac{m H_{\varphi c}^2}{4\pi \rho_c k T_c} \sim 2 \times 10^{-6}$. We can note that the descending flow from the pole results in a very small lowering of the temperature above the core. These laws are approximately accurate for $r > 1.2 r_c$ and $5° \leqslant \theta \leqslant 30°$.

Even though not exactly in the same context, Nucci & Busso (2014, Figure 2 and Equation (17)) grossly suggests similar simple scaling laws for the evolved AGB star's convective

---

[1] Only the the numerical coefficients result from the fitting, the litteral terms stem from dimensional analysis.

envelope (without the correcting terms proper to the dynamo region which is not considered by these authors). However, there exists an important difference for the circulation which decreases as a function of r in our model but is increasing in their work.

Starting from these laws, a semi-analytical model is certainly possible at least for the polar vortex (the dynamo area). The great interest of a semi-analytical model would be to skirt the numerical simulations which are hugely time-consuming.

Let us notice that the rotational law is perturbed but just a slightly by the presence of the magnetic field (compared to the initial simple law in r^{-2}). The decrease of the gradient of differential rotation due to the presence of the magnetic field is low. A steady polar dynamo thus takes place and this one is expected to last for a period of at least 5×10^3 yr (a very short period before the totality of the AGB phase and what could be constitute the final stage with a massive expulsion of matter). This period corresponds to the ejection of the totality of the convective envelope with mass loss $\sim 10^{-4} M_\odot \, {\rm yr}^{-1}$. A shut-down of the meridional circulation would obviously lead to a cut off of the dynamo. If the first ingredient for the dynamo is the presence of a polar vortex, a stable meridional circulation is the central piece to sustain this dynamo. This circulation has also to be in the right sense (the polar vortex is constantly fed with fresh angular momentum by the meridional circulation). Seen from the core surface the matter rises at the equator and sinks near the pole axis. Without these two essential conditions (a polar vortex and a meridional velocity taken in the right sense) the dynamo does not run. On the other hand it is very difficult to know if such a phenomenon can last for 10^4 yr. We note that the presence of a meridional circulation is also attested in the Sun (where besides the same intricate problems to solve are encountered).

The magnetic field is maintained at such a moderate level ($H_{\varphi c} \sim 10^6$ Gs) owing to the high flux loss along the equatorial plane which evacuates the field.[2] Clearly the field is rapidly created by a polar dynamo and the equatorial evacuation insures a steady state (for at least a period of 10^4 yr which is indeed a short period before the total duration of the AGB stage). Jordan et al. (2012) have shown that the magnetic field of central stars of PNe is weak. In fact when the evolved AGB envelope is ejected, the dynamo mechanism described here simply disappears together with the envelope. A refined analysis of our results near the surface of the degenerate core

---

[2] Let us specify that the term of "flow" of magnetic flux would be more adequate because the term "loss" seems to suggest that the magnetic field is destroyed. It is not the case. The flow of magnetic flux is conservative. It is well known for a long time that the turbulent diffusion is unable of significant destruction of magnetic fields in a star (the turbulence is quenched by the magnetic field at a small scale well above the molecular level where destruction by ohmic diffusion is indeed possible, but this one is negligible here), see for instance Vainshtein & Rosner (1991). Eventually it is experimentally proven that turbulence can even reduce the magnetic diffusivity and concentrates the field (Cabanes et al. 2014).

shows that the azimuthal magnetic field lines slide on this surface and that the poloidal component is not anchored to it. The magnetic field of the core could even be null. The idea that the magnetic field of the central stars of CSEs is linked to that of their surrounding CSEs must be give up.

Near the core surface the magnetic field is quasi azimuthal $\sim 10^6$ Gs. The temperature slightly increases and the density decreases toward the equator following the fitting laws

$$\rho \simeq \rho_c(1 + \delta \sin^2 \theta) \quad T \simeq T_c(1 + \beta + \gamma)(1 + \epsilon \sin^2 \theta)$$

(15)

with $\delta = -\frac{mv_c^2}{2kT_c} \sim 4 \ 10^{-5}$ and $\epsilon = 9\frac{mv_c^2}{2kT_c} \sim 4 \ 10^{-4}$.

The magnetic field is also quasi-azimuthal in the equatorial plane. It is strongly concentrated in a thin disk (with a noticeable uniformity guided by the meridional rollers which squeezed the disk) where the diffusivity is very low. The density deviation within the disk with respect to the field-free surroundings is weak $\delta\rho/\rho \sim 4 \times 10^{-5)}$, but this effect is sufficient to insure the natural uplift of the matter opposing a positive force to the retraction force of the magnetic field lines.

We can also note that the energy distributed in the meridional circulation $\rho v^2 \sim 10^{11}$ erg cm^{-3} and in the magnetic fields $H^2/8\pi \sim 10^{11}$ erg cm^{-3} in the core region are weak before the gravitational energy $GM_c\rho/r_c \sim 10^{16}$ erg cm^{-3} (magnetic intensity equivalent $\sim 7 \times 10^8$ Gs). Both the meridional circulation and magnetic fields only very little affect the core region equilibrium.

The density distribution remains spherical in the convective envelope excepting in the region where a strong azimuthal magnetic field is present (but the deviation is $\frac{\delta \rho}{\rho}$ is very weak $\sim 4 \times 10^{-5}$).

The disk remains thin up to 3×10^{12} cm. Its thickness slowly increases as $r^{0.58}$ and otherwise the field decreases as $r^{-0.66}$. The transport from the core up to this distance takes ~ 25 days. During this transport the orthoradial balance between the disk and its surroundings is checked. At the same time, the ratio of magnetic energy to thermal energy within the disk drastically increases from a very weak value $\sim 10^{-5}$ to ~ 1. The fact that the field is not diffuse but remains concentrated during the transport is a very happy situation because a diffuse (and therefore weak by flux conservativity) field would not supply an efficient mechanism for the ejection of gas and, furthermore, it appears especially difficult to concentrate a diffuse field at the surface. Very similarly the observations at the surface of the Sun show that the solar magnetic field appears to occur not in a diffuse configuration but rather in small-scale concentrations of very high intensity.

On the other hand while the disk is quasiuniform, at both of its boundary surfaces the magnetic field is weak and can be manipulated by turbulence at small scale with bubbles emerging in the free-field medium. Subsequently the uplift of the disk must be accompanied by an orthoradial mass loss (may

be following a process similar to the loss of plasma by the coronal holes at the surface of the Sun see Parker 1984). Unfortunately this lateral mass flux is very difficult to quantify and this is left as a free parameter. Let us specify that this phenomenon is not accompanied by a concomittant net lateral magnetic flux loss because the magnetic field lines in the bubbles which randomly rotate become diversely oriented and mutually annihilate (see for instance Vainshtein & Rosner 1991, especially their Figure 1). Very likely other mechanisms which concentrate the magnetic field during the transport up to the surface are possible (Brandenburg et al. 2016). The radial flow of magnetic flux in the disk is conservative (i.e., $\dot{\Phi}$ is constant). If one relaxes the axisymmetry hypothesis, that is taking into account of the φ-dependence, the disk could undulate during the transport but the analysis of such a phenomenon requires to work in the framework of a 3D model and a supercomputer is needed.

A very compelling result of this model is that starting with solar values at the beginning of the calculations, and after of while, waiting up to the installation of a steady state, we obtain a flux loss $\phi \sim 10^{20}$ Mx s^{-1} which is typical of magnetic flux observed in CSEs (for a CSE with a mean radius of 10^{16}–10^{17} cm and a mean velocity of 10 km s^{-1} a mean magnetic field of 10^{-3} Gs (observational data) the flux is $\phi = 10^{19}$–10^{20} Mx s^{-1}. Is it a coincidence?). This statement strongly supports the proposed model: it is then tempting to assume that a single star with a solar mass is able to produce at the tip of the AGB phase the magnetic field flux observed in CSEs of evolved stars. We can note that this machinery can also run with a wide binary star but may be with interesting addition of precessional effects very often invoked by observers of PNe (Balick et al. 2001).

b. The evolved AGB envelope-superwind transition area

We have introduced a so-called "transition zone" which begins at $r = 3 \times 10^{12}$ cm. This terminology, has been already considered earlier in the text as a mesh division, but also calls for a physical explanation. This zone is part of the convective envelope and is defined as follows. Near the core surface the ratio of the magnetic pressure, P_{mag}, to thermal pressure, P_{th}, is of the order of 10^{-5}. The magnetic field plays a little role in the vicinity of the core surface. In the inner part of the convective envelope the thermal pressure approximately decreases as $r^{-\frac{5}{2}}$ while the magnetic pressure decreases more slowly as $r^{-1.3}$ (the magnetic field is squeezed in the equatorial plane by the rolling mills action of the meridional circulation). We arbitrarily fix the base of the "transition zone" where $\frac{P_{mag}}{P_{th}} \sim 10\%$. When approaching the surface of the star this ratio still continues to increase and the magnetic pressure becomes comparable to the thermal pressure, which ultimately leads to an MHD ejection.

The "surface" of the evolved AGB star is not a so well defined simple geometric shape. Rather it is a "volume" which extends from 3×10^{12} to 3×10^{13} cm. The boundary
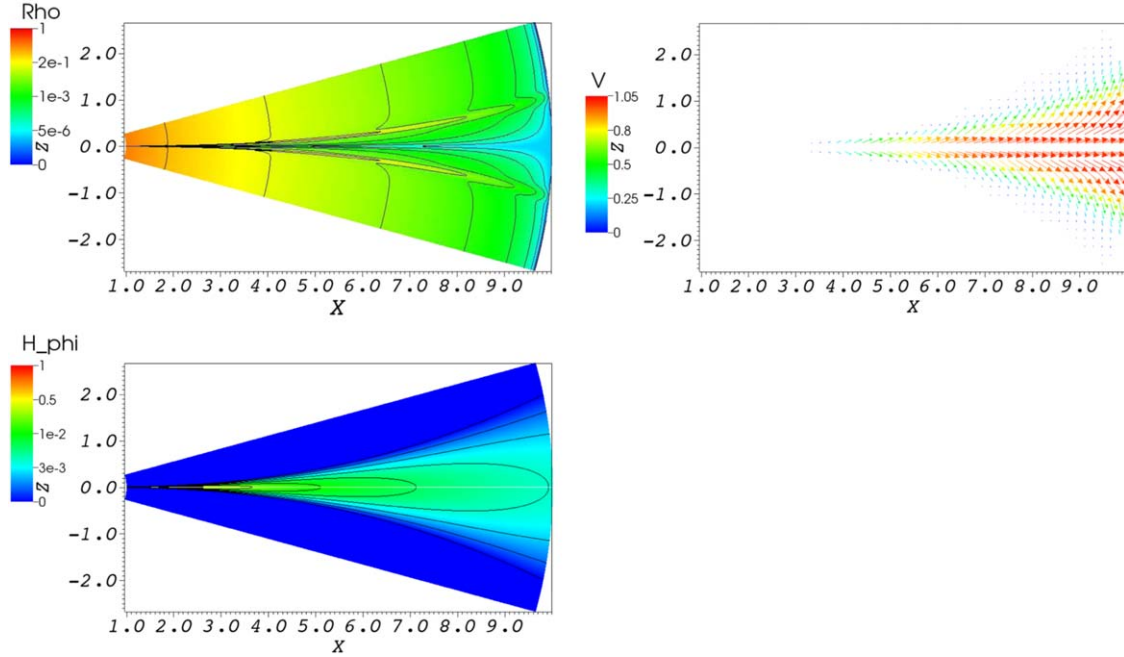
Figure 5. (a) Star-superwind transition area: surface and contour plots of the density ρ in normalized units, unit $= 5.3 \times 10^{-7}$ g cm^{-3} (log scale). The unit of distance is 3×10^{12} cm. (b) Star-superwind transition area: velocity field in normalized units (unit $= 30$ km s^{-1}). (c) Star-superwind transition area: surface and contour plots of the magnetic field H_φ in normalized units, unit $= 2.3 \times 10^3$ Gs (log scale).
(A color version of this figure is available in the online journal.)

conditions at $r = 3 \times 10^{12}$ cm are $\rho_e = 5.3 \times 10^{-7}$ g cm^{-3}, $H_e = 0$ in the evolved AGB's envelope and ρ_i is left undetermined (for $\rho_i = \rho_e/2$, a mass loss much higher than $\sim 10^{-4} M_\odot$ yr^{-1} could be reached), $H_i = 5 \times 10^3$ Gs (by conservativity of magnetic flux) in the thin disk. Only a narrow equatorial band is concerned with angles between $-15°$ and $15°$. For both these sides the conditions of the static envelope have been prescribed. A reflective condition is assigned at $\theta = 0$. At $r = 3 \times 10^{13}$ cm the boundary conditions are obviously free (the software determines them itself and these conditions are later chosen at the base of the superwind, except the mass loss fixed to $\dot{M} \sim 10^{-4} M_\odot$ yr^{-1}. The conservativity of the magnetic flux is simply checked. The steady solution has been found by trial and error up to convergence starting from rescaled preceding results (Pascoli & Lahoche 2010). The Figures 5(a)–(c) supply respectively the density, the velocity field and the magnetic field in the transition zone.

The velocities at the outlet of the nozzle ($r \sim 3 \times 10^{13}$ cm) are moderately high ~ 35 km s^{-1}. They are found to be 16% above the liberation velocity (30 km s^{-1}). We can see that both the gas density and the frozen-in magnetic field intensity very rapidly decrease on a scale height $\sim 3.2 \times 10^{12}$ cm. The area under examination acts similarly to an usual MHD nozzle where the kinetic energy increases at the expense of the magnetic energy, the flowing gas going from a super-alfvenic regime to a sub-alfvenic one. The gradient of density is severe

in this area leading to a strong turbulence and any kind of instabilities. On the other hand the velocities are large and the expansion is adiabatic. The mean temperature decreases from $\sim 4.5 \times 10^4$ K and reaches ~ 100–200 K at the the base of the superwind. The gas emitted at the base of the superwind is thus cold as due to the adiabatic expansion.

We have shown in the present study that at least a steady and laminar solution is existing. However, a gentle laminar flow is an indealized situation, a lot of work remains to be done to understand how exactly the magnetized disk pierces the stellar envelope and reaches the surface. A time-dependent model is needed for that but the main difficulty is the treatment of the numerical instabilities (given the very high degree of stratification in density).

There also exists a lot of physical instabilities which appear when a magnetic field is present: the magnetic field can for instance possibly produce in this area a delicate small-scale filamentary structure in the form of twisted ropes (these twisted ropes indeed are ubiquitous and have been identified at the surface of the Sun in the corona, but also in many parts of the solar system, the ionosphere of planets, etc., even though their origin is still controversial. These twisted ropes can form by shearing motion, convergence flow, etc, see for instance, Priest & Longcope 2017). There too a 3D analysis is needed, however, we are insured that it is under this form that the magnetic field appears at the base of the superwind.

We see very often in the literature that the authors conclude from their observations that the (mean) magnetic field is of the order of ~ 10 Gs at the surface (without quotation marks) of an evolved AGB star. In fact this point of view must be corrected. At the surface of an AGB star the magnetic field is very likely near zero. The intensity deduced from the observations is that taken at the base of the superwind (the top of the "surface" of the evolved AGB star with quotation marks). Nucci & Busso (2014) use a mean intensity $\gtrsim 3$ Gs in their calculations. However, such a mean value seems high. In our calculations we find a mean intensity scattered on the evolved AGB star's surface of the order of 1 Gs. In fact this quantity is fictitious given the field is not scattered but appears concentrate in an equatorial belt. In anyway the important item is not the intensity of the magnetic field, but the magnetic flux loss which is imposed by the capacity of the core region to produce such a flux. Furthermore the star is hidden from view of observers by a surrounding thick disk where the magnetic field is estimated to 1 Gs.

M_c	$M_{\rm env}$	Ω_c (s^{-1})	$\dot{M}$ ($M_\odot$ yr^{-1})	$\dot{\Phi}$ (Mx yr^{-1})
0.5	0.5	0.01	10^{-4}	6×10^{27}

The ejection duration is very grossly fixed by the total mass of the evolved AGB's envelope, even though the phenomenon would need a very prohibitive CPU time to be fully visualized from the beginning to the end.

According to the present model, with calculated mass loss $\dot{M} \sim 10^{-4} M_\odot$ yr^{-1} and flux loss $\dot{\Phi} \sim 3 \times 10^{27}$ Mx yr^{-1} (against respectively $\dot{M}_\odot \sim 2$–$3 \; 10^{-14} M_\odot$ yr^{-1} and $\dot{\Phi}_\odot \sim 10^{22}$–$10^{24}$ Mx yr^{-1} for the Sun), the duration of the phenomenon amounts to $\sim 5 \times 10^3$ yr. Varying the parameter Ω_c by a factor x, gives $\dot{M} \sim 10^{-4} \times x^2 \; M_\odot$ yr^{-1} and $\dot{\Phi} \sim 3 \times 10^{27} \times x$ Mx yr^{-1}; then this duration is modified by a factor x^2 for the same total mass of the evolved AGB's envelope. However, the value of Ω_c is linked to the initial mass of the star and thus to the mass of the evolved AGB's envelope itself.

(c) The CSE

The area under study extends here from 3×10^{13} to 3×10^{15} cm. The boundary conditions are specified at the base of the superwind assumed to be located at $r = 3 \times 10^{13}$ cm and derived from the results of the transition area. At the base of the superwind (i.e., 3×10^{13} cm) the boundary conditions are $\rho_w = 2 \times 10^{-12}$ g cm^{-3} and $H_w = 10$ Gs. The boundary conditions at $r = 3 \times 10^{15}$ cm are left free. The Figures 6(a), (b) and 7(a), (b) supply the density and magnetic field in the CSE. As shown in Figure 6, in the circumstellar area surrounding the star, the matter is preferentially ejected in a definite plane with formation of a equatorial thick disk surrounding the star (thikness $\sim 3 \times 10^{13}$ cm). This region is labeled by 1 in Figure 6(b)). The magnetic field remains relatively concentrated in the equatorial plane with the

development of a thick disk. This disk is then continuously extended by a horn toward higher latitudes, the latter one being then interrelated to the bipolar jet (Figures 6(a) and (b)) (see the figures published in the literature: M2-9 Schwarz et al. 1997, He 2-320 and He 3-401 Sahai 2002). Besides, an analysis of the results now reveals that between r_* and $10 \; r_*$ the superwind is not radial but the matter is strongly deviated toward the higher latitudes. The density varies as $r^{-5/2}$ and the magnetic field as $r^{-3/2}$ in this area. Beyond $r \sim 50 \; r_*$ the motion is quasi-radial $\rho \sim r^{-2}$ and $H \sim r^{-1}$ and the gas distribution becomes quasi-isotropic but with a concentration in the polar regions in the form of long and very directive jets (these jets can however evolve toward a kind of "snake" by instability). We can thus conclude that the inner anisotropies (disk, barrel structure and jets) are hidden from the observer view by the outer more spherical regions. This fact could explain why the CSEs appear approximately round at an early stage, even though the ejection process is clearly asymmetrical.

The modelization of the strictly speaking PN's phase deserves a further examination. The polar holes labeled by 2 in Figure 6(b) must play an important role in the morphology of PPNe and PNe. When the degenerate core is exposed after the ejection of the evolved AGB's envelope, the hot gas pushes the dense gas of the CSE. The effect of bulldozing is differential, following the direction taken into account. The polar cavities with very low density offer lesser resistance than in the equatorial plane direction (in this plane a thick torus is formed by compression) and the hot gas can pick up in them creating two bubbles on each side of the equatorial thick torus with appearance of a typical bipolar PN.

Each cavity (north or south) is itself topped above by a polar jet (labeled by 4 in Figure 6.2). This jet is produced by a magnetic striction effect as early suggested (Pascoli 1992; García-Segura et al. 1999). The confinement is well visible in NGC 7009 where the jets are very thin and straight (one jet ends up by an umbrella). Even though the present model always implies the formation of these polar jets, there exists two types on PNe. Some PNe possesses very prominent polar blobs and likely built-up from compression of polar jets (e.g., NGC 650-1, NGC 4242, NGC 6826, NGC 7009, NGC 3471/2), while on the contrary in others PNe these blobs are lacking at the extremities of the symmetry axis (assuming a prolate configuration: e.g., NGC 6720 and NGC 7293 Pascoli 1990a, 1990b).[3] It seems that in some objects the polar structures are reinforced, and by contrast in others ones the blobs are eroded by the fast wind and/or the radiation field emitted by the central star at an evolved stage.

At a circumstellar stage we see just the outer regions and the envelope appears round as observed (we can also note that the

---

[3] There is also the very atypical case of the Red Rectangle nebula which is not barrel-shaped but strangely cone-shaped. However, in this unusual case a binary star as progenitor could be clearly involved in the shaping mechanism.
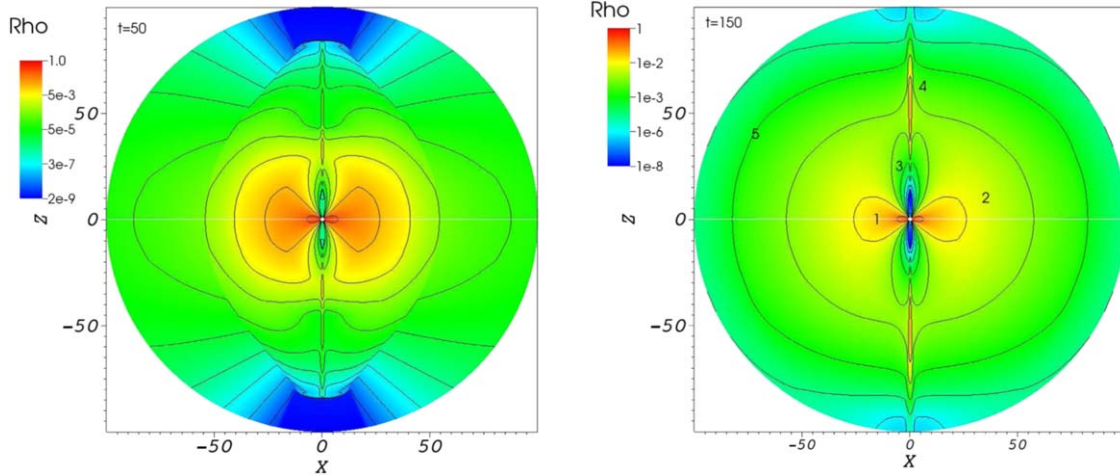
Figure 6. Circumstellar envelope: surface and contour plots of the density ρ in normalized units, unit $= 2 \times 10^{-13}$ g cm^{-3} taken in the disk (log scale). The unit of distance is the radius of the star $r_* = 3 \times 10^{13}$ cm. The time unit is 100 days.
(A color version of this figure is available in the online journal.)

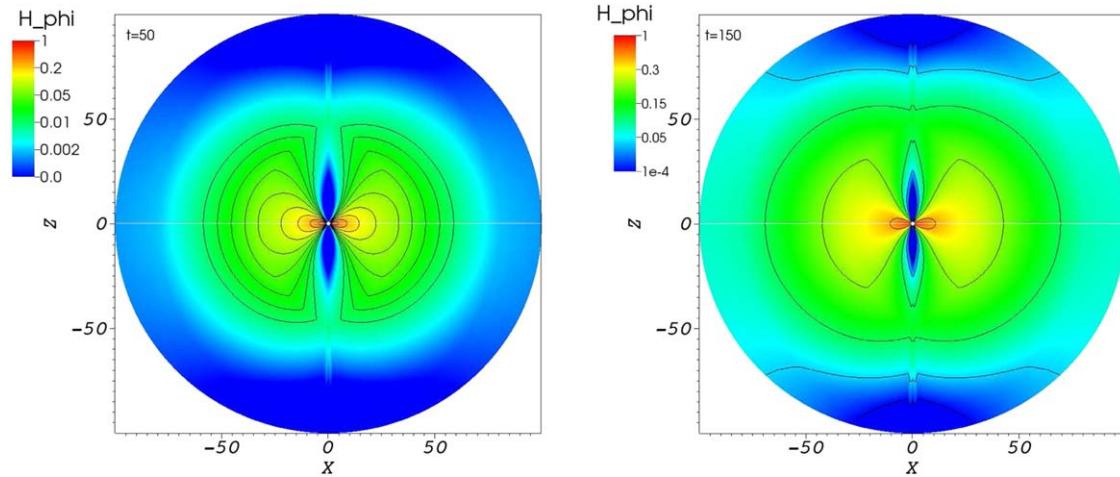**Figure 7.** Circumstellar envelope: surface and contour plots of the magnetic field H_φ in normalized units, unit $= 1$ Gs taken in the disk (log scale). The unit of distance is the radius of the star $r_* = 10^{13}$ cm. The time unit is 100 days.
(A color version of this figure is available in the online journal.)

magnetic field appears very coherent on a large scale). This is contrasting with the delicate structures which is hidden in the inner regions. Following the considerations above a CSE must be a very complex object indeed. Even though the ejection process is continuous (one single ejection is assumed), we mainly distinguish five structures labeled by the numbers reported in the Figure 6(b):

(1) A disk surrounding the star.
(2) A barrel-shaped structure with more or less pronounced filaments.
(3) Polar holes inside the barrel-shaped structure.

(4) A polar jet above each hole piercing the barrel-shaped substructure.
(5) A quasispherical envelope in the outer region which masks the inner structures excepting the extremities of the polar jets.

We can point out that in the present scenario, all these structures derive by inflation of a magnetized disk emitted by the central star and not from a bipolar outflow. The bipolarity is shaped after the ejection by long-range Lorentz forces. On the other hand the fast wind emitted when the degenerate core is exposed is very likely spherical.
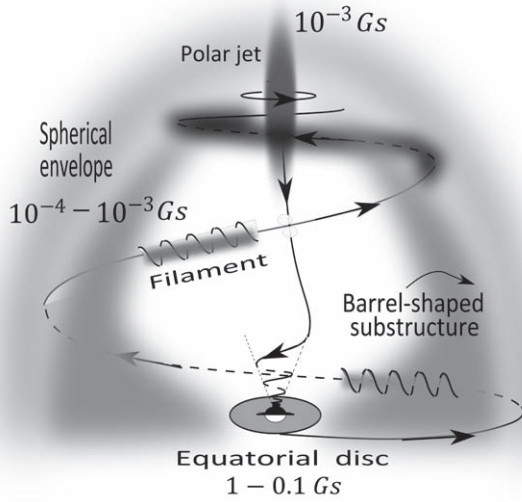
Figure 8. Synoptic view of a magnetic bundle in a circumstellar envelope. The barrel-shaped structure is hidden by a quasi-spherical envelope (sketch from Figure 6(b)). The core is also reported (not to scale). Circumstellar envelopes evolve in PNe which keep still track of their origin, see by comparison NGC 3242, NGC 6826, NGC 7009 and NGC 6843 from the *Hubble Telescope*. In NGC 7009 we can see the confined jets (the so-called streams in Sabbadin et al. 2004) and their clear links with the barrel-shaped structure.

A magnetic field line is continous and without boundary (a piece of magnetic filament with two extremities is obviously unphysical). It must be a closed path even if this path is not a single loop but can be very interlaced. What is the fate of a magnetic filed line in an evolved AGB star-CSE system? We show in Figure 8 the full path of such a line (only one hemisphere is shown). It goes from the core of the evolved AGB star to the nebula by the equator and returns to the core by the polar axis. This line can draw in the body of the nebula a clelia. Let us notice that the magnetic field entering by the pole in the star is radial ($H_r < 0$). By conservation of flux, this signifies that the field in the equatorial plane is not purely toroidal but possesses a small pitch angle with $\frac{H_r}{H_\varphi} \sim 0.1$ and $H_r > 0$. A piece of twisted rope is also shown, undoubtedly built-up in the transition area (sole a small piece is shown but in fact by continuity of the carried-current it is all the magnetic field line which must exhibit such a twisted structure).

If the gas is not homogeneous but filamentary, a very likely situation when a magnetic field is present, a bundle of magnetic lines could be more prominent than others and could directly be visualized. Some nebulae seems to exhibit such substructures accompanied of filamentation effects (Huggins & Manley 2005). However, a comparison with a composite image of NGC 6543 (the famous Cat's Eye nebula) suggests that the polar jet might not stay straight as represented here, but rather could undergo a kink deformation. Thus one of the two symmetric jets in the Cat's Eye nebula is broken at right angle

(if this is due to the presence of a magnetic field, we have an instability in the azimuthal mode $m = 1$). We can observe the same kink effect on a very prominent filament in M2-9. By the way it seems difficult to explain such a net symmetry breaking by a contiuous precession of a binary nucleus. We observe a second type of instability in the opposite jet which is divided into two secondary separate jets (instability in the filamentation modes $m \geqslant 2$). We can also note the strinking resemblance between NGC 6543 (the Cat's eye) and NGC 7009 (the Saturn nebula): multiple concentric thin shells, small scale filaments and bipolar jets. In the latter one we can see one of the jets with a thread-like structure ended with a stagnation point at its tip (to be compared with the Figure 4 of Bellan 2018). There also exists a very conspicuous and intriguing braid composed of thin twisted ropes well visible in a lobe of M2-9, a phenomenon which is very difficult to explain without the presence of a magnetic field but easy with it. Some types of these plasma instabilities are described in Ciardi et al. (2009), Bellan (2018) and papers quoted therein, even though an extrapolation of laboratory experiments to astrophysical objects must be taken with cautious, and the very large scale difference (especially concerning the characteristic timescale for the magnetic diffusivity) must be keep in mind.

For the very complex and archetypal nebula M2-9 which seems to bring together all the difficulties, other interpretations has also been proposed with both a binary star progenitor and periodic mass ejections (Balick et al. 2001). There is a remarkable series of outer, evenly spaced, spherical shells of gas. The duration between each ejection (in the framework of a multiple shell ejection) is rather surprisingly stable and of the order of 1000 yr. However, this period is very different from that linked to thermal pulses $\gtrsim 10^4$ yr (Lau et al. 2012) or to pulsations of evolved AGB stars ~ 1 yr (McDonald et al. 2018). The apparent absence of turbulence in these concentric envelopes is also troublesome. A simple suggestion is that this turbulence could be cut off by a large-scale magnetic field in the short wavelength range and the energy generated by a shock would be then stored in wavelengths of the order of the distance between the shells. However, this idea is very difficult to treat from a theoretical point of view. Another idea will be to see this series of concentric envelopes as a soliton train, well known in many contexts such as undular bores and whelps in hydrodynamics and meteorology, where the magnetic striction would play the role of the usual gravity, completely negligible here. More generally, in light of the present model, we hypothesize that this multiple shell structure could possibly have an in situ origin in the spherical envelope (the descendant of the round CSE surrounding the barrel-shaped substructure). Magnetic instabilities can directly act within the spherical envelope, all the phenomena taking place in the framework of a continuous and unique flow of gas without appeal to an abrupt change in the mode of ejection. On the other hand the geometry of this strangely sliced spherical envelope exhibits a very

impressive contrast with the inner region which is clearly strongly axisymmetric. A contrario in the scenario of a multiple ejection process what could be the cause of this very sudden regime change from a near perfect spherical mode to an axisymmetric one during the superwind phase without any change of the gas chemical composition?

Let us eventually notice that the Cat's Eye is also surrounded by an enormous spherical (but very faint) envelope (Corradi 2004). This outer envelope is composed of a complex network of interlaced filaments whose the morphology presents strong similarities with the Crab Nebula where a magnetic field have been clearly identified ($\sim 10^{-4}$–10^{-3} Gs), and this even though the expansion velocities in these two distinct objects (a planetary nebula for the Cat'Eye with no synchrotron emission and a remnant of supernova for the Crab Nebula with synchrotron emission) differs by a factor 100.

Eventually as we have already aforementioned the big problem is that a simulation model is very-time consuming and costly. A semi-analytical model would be welcome (a bit like that of Nucci & Busso (2014), however, these authors did not consider either the dynamo mechanism, or the ejection process by the evolved AGB star. A partitioning of the study in different areas would be needed in this case.

5. Conclusion

We have succeeded in producing a self-consistent time-dependent MHD model of CSE ejection at the tip of the AGB phase. The present paper supplies new results compared to the preceding time-independent models of Pascoli & Lahoche (2010). We start with a spherical AGB star composed of a very huge convective envelope surrounding a small and dense degenerate core. After incorporating an angular velocity distribution, the symmetry is lowered in the core region, going from spherical to cylindrical. A meridional circulation then naturally appears. This circulation in turn produces a reshuffling of the angular velocity wich becomes polar. We predict the existence of a huge polar vortex above the degenerate core of an evolved AGB star. Above this degenerate core, fast angular velocities are then located at higher latitudes where a dynamo is operating. Magnetic fields are then amplified and stored away from the dynamo region toward the equatorial plane where a thin magnetized disk develops. A magnetic field of the order of 10^6 Gs is predicted just above the core. The disk rises later radially throughout the evolved AGB's envelope up to the "surface" by buoyancy. The magnetic field value at the "surface" is estimated at 10 Gs (the measurement is made in the zone where the wind is emitted, this giving a mean magnetic field (a fictitious value) at the surface of the AGB of $\sim$1 Gs. This ambiguity present in a lot of papers does that the concept of intensity should give way to that of magnetic flux which is much more relevant). In this framework the ejection of gas by the AGB star at its "surface" is MHD-driven. The mean

magnetic flux loss and the expansion velocity are predicted in good agreement with observational inferences ($\dot{\Phi} \sim 3\ 10^{27}$ Mx yr^{-1}), $v_e \sim 20$ km s^{-1}. The mean mass loss is more difficult to determine, but a mass loss $\dot{M} \sim 10^{-4} M_\odot$ yr^{-1} is easily obtained, comparable to the observational estimates. However, much higher mass loss could also be produced (as in the case of M2-9). The transition from a grossly round CSE toward the characteristic bona fide bipolar morphology of PNe has also been questioned. This noticeable morphology could result at a post-AGB stage, when the degenerate core is exposed. The shaping of the bipolarity is achieved starting from the hidden anisotropic distribution of matter buried in the inner region of the CSE. This question is left as a further work. Eventually to understand the surimposed filamentary structure, a 3D model taken into account of an azimuthal dependence for the physical quantities is required, but will need a huge amount of CPU ressources. More generally many interrogations relative to the existence of magnetic fields in the CSEs of evolved AGB stars and in PNe remain to be answered.

References

Balick, B., Wilson, J., & Hajian, A. R. 2001, AJ, 121, 354
Beck, R., Brandenburg, A., Moss, D., & Shukurov, A. 1996, ARA&A, 34, 155
Bellan, P. M. 2018, PhPl, 25, 055601
Blackman, E. G. 2009, in IAU Symp. 259, Cosmic Magnetic Fields: From Planets, to Stars and Galaxies, ed. K. G. Strassmeier, 35
Blackman, E. G., Franck, A., Markiel, J. A., Thomas, T. H., & Van Horn, H. M. 2001, Natur, 409, 485
Brandenburg, A., Kleeorin, N. I., & Rogachevskii, I. 2016, NJPh, 18, 125011
Busso, M., Gallino, R., & Wasserburg, G. 1999, ARA&A, 37, 329
Cabanes, S., Schaeffer, N., & Nataf, H. C. 2014, PhRvL, 113, 184501
Charbonneau, P. 2010, LRSP, 7, 3
Chatterjee, P., Nandy, D., & Choudhuri, A. R. 2004, A&A, 427, 1019
Chevalier, R. A., & Luo, D. 1994, ApJ, 421, 225
Ciardi, A., Lebedev, S. V., Frank, A., et al. 2009, ApJL, 691, L147
Corradi, R. 2004, https://www.spacetelescope.org/images/heic0414b/
Dikpati, M., & Charbonneau, P. 1999, ApJ, 518, 508
Dikpati, M., Choudhuri, A. R., & Schüssler, M. 1995, A&A, 303, L29
Dobler, W., Stix, M., & Brandenburg, A. 2006, ApJ, 638, 336
Duthu, A., Herpin, F., Wiesemeyer, H., et al. 2017, A&A, 604, A12
Ferrario, L., de Martino, D., & Gaensicke, B. 2015, SSRv, 191, 111
Fossat, E., Boumier, P., Corbard, T., et al. 2017, A&A, 604, A40
García-Segura, G., Langer, N., Róyczka, M., & Franco, J. 1999, ApJ, 517, 767
García-Segura, G., López, J. A., & Franco, J. 2005, ApJ, 618, 919
Gilman, P. A., & Rempel, M. 2005, ApJ, 630, 615
Guerrero, G. A., Muñoz, J. D., & de Gouveia Dal Pino, E. M. 2005, in AIP Conf. Proc. 784, Magnetic Fields in the Universe, From Laboratory and Stars to Primordial Structures (Melville, NY: AIP), 574
Gurzadian, G. A. 1969, Planetary Nebulae (New York: Gordon and Breach)
Habing, H. J. 1996, A&ARv, 7, 97
Herpin, F., Baudry, A., Thum, C., Morris, D., & Wiesemeyer, H. 2006, A&A, 450, 667
Herwig, F. 2005, ARA&A, 43, 435
Höfner, S., & Olofsson, H. 2018, A&ARv, 26, 1
Huggins, P. J., & Manley, S. P. 2005, PASP, 117, 665
Jordan, S., Bagnulo, S., Werner, K., & O'Toole, S. J. 2012, A&A, 542, A64

Jordan, S., Werner, K., & O'Toole, S. J. 2005, A&A, 432, 273
Karakas, A. I., & Lattanzio, J. 2014, PASA, 31, e030
Kemball, A. J., Diamond, P. J., Gonidakis, I., et al. 2009, ApJ, 698, 1721
Kerschbaum, F., Ladjal, D., Ottensamer, R., et al. 2010, A&A, 518, L140
Kitchatinov, L. L. 2016, Ge&Ae, 56, 945
Krause, F., & Rädler, K.-H. 1980, Mean-field Magnetohydrodynamics and
    Dynamo Theory (Oxford: Pergamon)
Küker, M., Rüdiger, G., & Schultz, M. 2001, A&A, 374, 301
Lau, H. H. B., Gil-Pons, P., Doherty, C., & Lattanzio, J. 2012, A&A, 542, A1
Lèbre, A., Aurière, M., Fabas, N., et al. 2014, A&A, 561, A85
Liang, Z.-C., Gizon, L., Birch, A. C., Duvall, T. L., Jr, & Rajaguru, S. P. 2018,
    A&A, 619A, 99
Matt, S., Balick, B., Winglee, R., & Goodson, A. 2000, ApJ, 545, 965
McDonald, I., De Beck, E., Zijlstra, A., & Lagadec, E. 2018, MNRAS,
    481, 498
Mignone, A., Bodo, G., Massaglia, S., et al. 2007, ApJS, 170, 228
Mignone, A., Zanni, C., Vaidya, B., et al. 2015, PLUTO User's Guide, v.4.2,
    (http://plutocode.ph.unito.it)
Neri, R., Kahane, C., Lucas, R., Bujarrabal, V., & Loup, C. 1998, A&AS,
    130, 1
Nordhaus, J., Busso, M., Wasserburg, G. J., Blackman, E. G., & Palmerini, S.
    2008, ApJL, 684, L29
Nordhaus, J. T., Blackman, E. G., & Franck, A. 2007, MNRAS, 376, 599
Nucci, A. M., & Busso, M. 2014, ApJ, 787, 141
Parker, E. N. 1984, ApJ, 281, 839

Pascoli, G. 1987, A&A, 180, 191
Pascoli, G. 1990a, A&AS, 83, 27
Pascoli, G. 1990b, A&A, 232, 184
Pascoli, G. 1992, PASP, 104, 305
Pascoli, G. 1997, ApJ, 489, 94
Pascoli, G., & Lahoche, L. 2008, PASP, 120, 1267
Pascoli, G., & Lahoche, L. 2010, PASP, 122, 1334
Patern, L., Sofia, S., & Di Mauro, M. P. 1996, A&A, 314, 940
Pipin, V. V., & Kosovichev, A. G. 2011, ApJ, 738, 104
Priest, E. R., & Longcope, D. W. 2017, SoPh, 292, 25
Rüdiger, G., & Hollerbach, R. 2004, The Magnetic Universe: Geophysical and
    Astrophysical Dynamo Theory (New York: Wiley), 343
Sabbadin, F., Turatto, M., Cappellaro, E., Benetti, S., & Ragazzoni, R. 2004,
    A&A, 416, 955
Sabin, L., Wade, G. A., & Lèbre, A. 2015, MNRAS, 446, 1988
Sabin, L., Zijlstra, A. A., & Greaves, J. S. 2007, MNRAS, 376, 378
Sahai, R. 2002, RMxAA (SC), 13, 133
Schwarz, H., Aspin, C., Corradi, R. L. M., & Reipurth, Bo. 1997, A&A,
    319, 267
Vainshtein, S. I., & Rosner, R. 1991, ApJ, 376, 199
Vlemmings, W. H. T. 2012, in IAU Symp. 283, Planetary Nebulae: An Eye
    to the Future, ed. A. Machado, L. Stanghellini, & D. Schönberner
    (Cambridge: Cambridge Univ. Press), 176
Vlemmings, W. H. T., van Langevelde, H. J., & Diamond, P. J. 2005, A&A,
    434, 1029